

Josephson effect in S/F/S junctions: spin bandwidth asymmetry vs. Stoner exchange

Gaetano Annunziata,¹ Henrik Enoksen,² Jacob Linder,² Mario Cuoco,¹ Canio Noce,¹ Asle Sudbø²

¹ SPIN-CNR, I-84084 Fisciano (Salerno), Italy

Dipartimento di Fisica “E. R. Caianiello”,

Università di Salerno, I-84084 Fisciano (Salerno), Italy and

² Department of Physics, Norwegian University of Science and Technology, N-7491 Trondheim, Norway

(Dated: November 8, 2018)

We analyze the dc Josephson effect in a ballistic superconductor/ferromagnet/superconductor junction by means of the Bogoliubov-de Gennes equations in the quasiclassical Andreev approximation. We consider the possibility of ferromagnetism originating from a mass renormalization of carriers of opposite spin, i.e. a spin bandwidth asymmetry. We provide a general formula for Andreev levels which is valid for arbitrary interface transparency, exchange interaction, and bandwidth asymmetry and analyze the current-phase relation, free energy, and critical current, in the short junction regime. We compare the phase diagrams and the critical current magnitudes of two identical junctions differing only in the mechanism by which the mid-layer becomes magnetic. We show that a larger number of $0 - \pi$ transitions caused by a change in junction width or polarization magnitude is expected when ferromagnetism is driven by spin bandwidth asymmetry compared to Stoner magnetism. Moreover, we show that these features can be present also for ferromagnets of the Stoner type having only a partial bandwidth asymmetry.

PACS numbers: 74.50.+r,74.45.+c,72.25.-b,74.25.Dw

I. INTRODUCTION

The antagonistic nature of ferromagnetism and singlet superconductivity notwithstanding, coexistence of these phenomena is not entirely ruled out and their interplay may in fact yield quite rich physics. Coexistence of ferromagnetism and superconductivity, predicted to occur in a phase where both the gauge and the continuous translational symmetries are spontaneously broken simultaneously,^{1,2} is suggested to emerge in many theoretical models.^{3,4} However, a decisive experimental verification of such coexistence is still lacking. On the other hand, the interplay between ferromagnetism and superconductivity in heterostructures has been the foundation for developments of numerous novel experimental techniques over the last decade or so.^{5,6} Besides the interest from a fundamental physics viewpoint, such systems hold potential in terms of future spintronics⁷ applications. The versatility of heterostructures involving superconductors and ferromagnets stems from the basic fact that Andreev reflections,^{8,9} processes taking place at the interfaces converting quasiparticles into Cooper pairs, are strongly affected by spin polarization.^{10,11}

In this paper, we focus on ballistic superconductor/ferromagnet/superconductor (S/F/S) Josephson junctions with conventional superconducting leads. These are systems capable of sustaining a supercurrent carried by Cooper pairs in the superconducting leads and by quasiparticles in the ferromagnetic mid-layer. The unique interplay between ferromagnetic and superconducting orders provides quasiparticles with extra phase shifts absent in junctions with a non-magnetic mid-layer. This can give rise to the appearance of a so-called “ π -phase”.¹² Under such circumstances, the energy minimum of the junction is reached at a phase difference of π across the junction, unlike the standard “ 0 -phase” in junctions with a non-magnetic mid-layer. The existence of the π -phase has been experimentally confirmed.^{13,14} As far as potential applications are concerned, π -junctions are consid-

ered to be candidates for realizing solid state qubits.¹⁵

Previous theoretical studies on S/F/S junctions^{16–25} have described the F layer using the Stoner model of metallic ferromagnetism, with oppositely polarized carriers occupying rigidly shifted bands. However, the interplay of Coulomb repulsion and the Pauli principle driving a metal into a ferromagnetic state,²⁶ may induce a *spin-dependent renormalization of the masses of charge carriers* with opposite spins, i.e. a spin bandwidth asymmetry. This mechanism appears in microscopic approaches where off-diagonal terms of Coulomb repulsion, generally neglected in studies based on the Hubbard model, are taken into account. A mean-field treatment of these contributions in addition to the exchange and nearest-neighbor pair hopping terms shows that quasiparticle energies for the two spin species are not simply splitted but get different bandwidths, i.e. effective masses. The net effect of these interactions is to render the hopping integral in the kinetic term spin dependent through bond charge Coulomb repulsion terms which are different for spin up and down carriers.²⁷ For low enough temperature and depending on Hamiltonian parameters, ferromagnetic order can be established only through this spin bandwidth asymmetric renormalization.²⁸ In this picture the ferromagnetism should be understood as kinetically driven, in the sense that it arises from a gain in kinetic energy rather than potential energy, unlike the usual Stoner scheme. We notice that this mass-split metallic ferromagnetism has been experimentally found to be the origin of the optical properties of the colossal magnetoresistance manganites,²⁹ of some rare-earth hexaborides³⁰ as well as of some magnetic semiconductors.³¹ Spin bandwidth asymmetry will substantially affect the coexistence of ferromagnetism and superconductivity,³² as well as the proximity effect³³ and transport in F/S bilayers.^{34,35} It is also responsible for an extension of the regime in which FFLO (Fulde-Ferrell-Larkin-Ovchinnikov) phase can be stabilized in heavy-fermion systems.^{36,37} In this work, we analyze the consequences of this

unconventional magnetism in ballistic S/F/S Josephson junctions by solving the Bogoliubov-de Gennes equations³⁸ for arbitrary spin polarization and interface transparency.

We show that bandwidth asymmetry in the F layer of a S/F/S junction modifies many physical properties such as Andreev levels dispersion, Josephson current and free energy. We provide a general formula for Andreev levels which holds for arbitrary interface transparency, exchange interaction, and bandwidth asymmetry and we calculate the corresponding Josephson current in the short junction regime for some important limiting cases. Comparing the results for a spin bandwidth asymmetry ferromagnet with those obtained for a conventional Stoner ferromagnet, we demonstrate analytically that the former manifests features that are only quantitatively different from the latter for low degrees of polarization. We show numerically that these differences become qualitative in the intermediate/high polarization regime. Then, evaluating the phase diagrams we infer that the mere mechanism by itself is able to shift the ground state superconducting phase difference from 0 to π or viceversa, with a spin bandwidth asymmetry ferromagnet tending to increase the number of possible $0 - \pi$ transitions in a fixed range of parameters.

This paper is organized as follows. In Section II, we introduce the model and notation, and provide a general formula for Andreev levels in S/F/S which is valid for arbitrary interface transparency, exchange interaction, and bandwidth asymmetry. In Section III we present an analytical form for Andreev levels and Josephson current in different limiting cases and numerically analyze the same quantities, critical current, and free energy for different polarization, temperature, F layer width, and interface transparency values. This analysis is performed considering both Stoner and spin bandwidth asymmetry magnetism in the F layer. The relationship between the spin polarization and the magnetic microscopic parameters is clarified by means of a general formula holding for a generic ferromagnet in which both mechanisms are present. In this “mixed” case, we also show that the features distinguishing pure spin bandwidth asymmetry from pure Stoner ferromagnets may exist even though the spin bandwidth asymmetry contributes only partially to spin polarization. We present phase diagrams and analyze $0 - \pi$ transitions which are driven by variations in the polarization and width of the F layer. The conclusions and a discussion on the applicability of our results to real materials is presented in Section IV, while analytical details for some quantities used in the paper are reported in the Appendices.

II. MODEL AND FORMALISM

We consider a ballistic Josephson junction composed of a ferromagnetic layer of width L sandwiched between two conventional s -wave singlet superconducting electrodes (see Fig. 1). Since the S electrodes are isotropic, we will consider an effective one dimensional model. Moreover, our results are

independent on the direction of the magnetic moment direction in F. The propagation of quasiparticles is described by

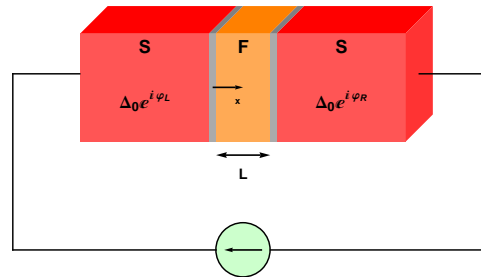


FIG. 1: A sketch of the current-biased S/F/S junction analyzed in the paper, along with notations that are used. The superconductors are treated as reservoirs, whereas the magnetic mid-layer has a finite width L .

the Bogoliubov-de Gennes equations³⁸

$$\begin{pmatrix} H_0^\sigma & \rho_\sigma \Delta \\ \rho_\sigma \Delta^* & -H_0^{\bar{\sigma}} \end{pmatrix} \begin{pmatrix} u_\sigma \\ v_{\bar{\sigma}} \end{pmatrix} = \varepsilon \begin{pmatrix} u_\sigma \\ v_{\bar{\sigma}} \end{pmatrix}, \quad \sigma = \uparrow, \downarrow, \quad (1)$$

where $\bar{\sigma} = -\sigma$, $\rho_{\uparrow(\downarrow)} = +1(-1)$, and $(u_\sigma, v_{\bar{\sigma}}) \equiv \psi_\sigma$ is the energy eigenstate in the electron-hole space associated with the eigenvalue ε . The single-particle Hamiltonian is

$$H_0^\sigma = H_L + H_F^\sigma + H_R + H_I, \quad (2)$$

where

$$\begin{aligned} H_L &= [-\hbar^2 \nabla^2 / 2m - E_F] \Theta(-x) \\ H_F^\sigma &= [-\hbar^2 \nabla^2 / 2m_\sigma - \rho_\sigma U - E_F] \Theta(x) \Theta(L - x) \\ H_R &= [-\hbar^2 \nabla^2 / 2m - E_F] \Theta(x - L) \\ H_I &= H [\delta(x) + \delta(x - L)]. \end{aligned} \quad (3)$$

Here, different effective masses m_σ for σ -polarized particles in the F layer, mimicking bandwidth asymmetry, has been included and U is the exchange interaction, E_F is the Fermi energy, $\Theta(x)$ is the Heaviside step function, m is the effective mass of the quasiparticles in the superconductors, and the parameter H quantifies scattering strength at S/F and F/S interfaces. We assume rigid superconducting order parameters with equal gap amplitude on both sides of the junction, i.e. $\Delta = \Delta_0 [e^{i\varphi_L} \Theta(-x) + e^{i\varphi_R} \Theta(x - L)]$, where $\varphi_{L(R)}$ is the phase of the left(right) superconductor. When considering finite temperature properties, we will assume the usual BCS dependence and let $\Delta_0 \rightarrow \Delta_0 \tanh(1.74 \sqrt{T_c/T - 1})$, where T_c is the superconducting critical temperature.

Employing the quasiclassical Andreev approximation,⁸ the solution of Eqs. (1) may be written as

$$\psi_\sigma(x) = \begin{cases} a_\sigma \begin{pmatrix} \rho_\sigma v \\ u \end{pmatrix} e^{ikx} + b_\sigma \begin{pmatrix} u \\ \rho_\sigma v \end{pmatrix} e^{-ikx}, & x < 0 \\ [\alpha_\sigma e^{iq_\sigma x} + \beta_\sigma e^{-iq_\sigma(x-L)}] \begin{pmatrix} 1 \\ 0 \end{pmatrix} + [\gamma_\sigma e^{iq_\sigma(x-L)} + \delta_\sigma e^{-iq_\sigma x}] \begin{pmatrix} 0 \\ 1 \end{pmatrix}, & 0 < x < L \\ c_\sigma \begin{pmatrix} u e^{i\varphi/2} \\ \rho_\sigma v e^{-i\varphi/2} \end{pmatrix} e^{ik(x-L)} + d_\sigma \begin{pmatrix} \rho_\sigma v e^{i\varphi/2} \\ u e^{-i\varphi/2} \end{pmatrix} e^{-ik(x-L)}, & x > L \end{cases}$$

where

$$u = \sqrt{\frac{\varepsilon + \sqrt{\varepsilon^2 - \Delta_0^2}}{2\varepsilon}}, \quad v = \sqrt{\frac{\varepsilon - \sqrt{\varepsilon^2 - \Delta_0^2}}{2\varepsilon}}, \quad (4)$$

and $k = \sqrt{2mE_F}/\hbar$, $q_\sigma = \sqrt{2m_\sigma(E_F + \rho_\sigma U)}/\hbar$ are Fermi wavevectors in the S and F electrodes respectively, and $\varphi = \varphi_R - \varphi_L$. The coefficients $a_\sigma, b_\sigma, c_\sigma$, and d_σ are the probability amplitudes for Andreev reflection as a hole-like quasiparticle (HLQ), normal reflection as an electron-like quasiparticle (ELQ), transmission to the right electrode as an ELQ, and transmission to the right electrode as an HLQ respectively, while the coefficients $\alpha_\sigma, \beta_\sigma, \gamma_\sigma$, and δ_σ are associated with right- and left-going ELQ and HLQ propagating through the ferromagnetic layer. All these probability amplitudes can be calculated by solving the linear system resulting from the boundary conditions

$$\begin{aligned} \psi_\sigma(0_-) &= \psi_\sigma(0_+) \\ \psi_\sigma(L_-) &= \psi_\sigma(L_+) \\ -\frac{2H}{\hbar^2} \psi_\sigma(0) &= \frac{1}{m} \psi'_\sigma(0_-) - \left(\frac{1}{m_\sigma} \right) \psi'_\sigma(0_+) \\ -\frac{2H}{\hbar^2} \psi_\sigma(L) &= \left(\frac{1}{m_\sigma} \right) \psi'_\sigma(L_-) - \frac{1}{m} \psi'_\sigma(L_+), \end{aligned} \quad (5)$$

which are valid for a general ferromagnetic electrode displaying both exchange splitting and bandwidth asymmetry. When the latter mechanism is present, electron- and hole-like parts of the wave function derivatives have to be joined separately with different masses. This is analogous to the situation where the insulating barriers are polarized with magnetic moment parallel to the one in the F layer and thus act with different strength on particles with opposite spin.³⁹ When only exchange splitting is present, i.e. $m_\sigma = m_{\bar{\sigma}} = m$, the usual form of the boundary conditions is recovered.¹⁷

Inserting the wave function into the boundary conditions, we obtain a homogenous system of linear equations for the scattering coefficients. By imposing that the system has non-trivial solutions, we can obtain a relation between energy and phase difference such that the coherent subgap processes can effectively take place, i.e. Andreev levels with dispersion $\varepsilon_i(\varphi)$, $i = \{1, \dots, 4\}$.⁴⁰ We are able to provide a general form of the levels which holds for arbitrary transparency of the insulating barriers, polarization in the ferromagnetic layer, and relative weight of the exchange and bandwidth asymmetry contributions. We find $\varepsilon_i(\varphi) = \varepsilon_\sigma^\pm(\varphi) = \pm \varepsilon_\sigma(\varphi)$ and

$$\varepsilon_\sigma(\varphi) = \Delta_0 \sqrt{\frac{A^2 + B^2 - A(C + D \cos^2(\varphi/2)) + \rho_\sigma \sqrt{B^2 (A^2 + B^2 - (C + D \cos^2(\varphi/2))^2)}}{2(A^2 + B^2)}}, \quad (6)$$

where A, B, C, D depend on all junction parameters. Their explicit form will be given in the Appendix A. Here, we merely note that for transparent interfaces, and in the absence of exchange field and bandwidth asymmetry, Eq. (6) reduces to the well known result $\varepsilon = \Delta_0 \cos(\varphi/2)$.⁴¹

We will focus on the short junction regime, i.e. $L \ll \xi$ where ξ is the superconducting coherence length, such that the Josephson current can be estimated by only considering

subgap contributions by Andreev levels^{40,42} as

$$\begin{aligned} I(\varphi) &= \frac{2e}{\hbar} \sum_i f(\varepsilon_i) \frac{d\varepsilon_i}{d\varphi} \\ &= -\frac{2e}{\hbar} \sum_\sigma \tanh\left(\frac{\beta\varepsilon_\sigma}{2}\right) \frac{d\varepsilon_\sigma}{d\varphi}, \end{aligned} \quad (7)$$

where $f(x)$ is the Fermi-Dirac distribution function and $\beta = 1/k_B T$.

Finally, the critical current is defined as $I_c = \max|I(\varphi)|$ and the phase of the junction (0 or π) is determined by the

minimum of the φ dependent part of the free energy

$$\begin{aligned}
 F(\varphi) &= -\frac{1}{\beta} \ln \left[\prod_i \left(1 + e^{-\beta \varepsilon_i(\varphi)} \right) \right] \\
 &= -\frac{1}{\beta} \sum_{\sigma} \ln \left[2 \cosh \left(\frac{\beta \varepsilon_{\sigma}(\varphi)}{2} \right) \right]. \quad (8)
 \end{aligned}$$

III. RESULTS

In this section we analyze Andreev levels, current-phase relation, free energy, and critical current for a short S/F/S junction. Our model enables us to take into account both bandwidth asymmetry and exchange interaction in the F layer. Defining the polarization as $M = (n_{\uparrow} - n_{\downarrow}) / (n_{\uparrow} + n_{\downarrow})$ and integrating densities of states as calculated from the H_F^{σ} term in Eq. (3), we find that in one dimension and at $T = 0$:

$$M = p_{+}/p_{-} \text{ with } p_{\sigma} = -\rho_{\sigma} \left[1 - \rho_{\sigma} \sqrt{\frac{m_{\uparrow} (1 + U/E_F)}{m_{\downarrow} (1 - U/E_F)}} \right]. \quad (9)$$

For a fixed value of the exchange splitting U , the effect of mass mismatch is to enhance the net polarization for $m_{\uparrow} > m_{\downarrow}$, and to hinder it the other way around. Eq. (9) describes a general F where both exchange and bandwidth asymmetry are present. We notice that Eq.(9) reduces to the case where only exchange interaction is present when $m_{\uparrow}/m_{\downarrow} = 1$ and $U \neq 0$ or the case where only bandwidth asymmetry is present when $m_{\uparrow}/m_{\downarrow} \neq 1$ and $U = 0$. We will refer to these two cases as a Stoner ferromagnet (STF) and a spin bandwidth asymmetry ferromagnet (SBAF), respectively. When both mechanisms are present there are several combinations of exchange energy and mass ratio that give the same polarization M . We choose to describe this mixed case through a parameter $W \in [0, 1]$ which quantifies the relative weight of the two mechanisms without changing the total polarization in such a way that a pure STF and a pure SBAF will correspond to $W = 0$ and $W = 1$, respectively. The detailed procedure chosen to calculate the value assumed by exchange and mass mismatch for a given polarization M and degree of mixture W is illustrated in Appendix B. In Table I, the magnetic parameter values for a STF, a SBAF, and a mixture of the two with $W = 0.5$, are reported for three values of the polarization $M = \{0.25, 0.50, 0.75\}$. Different Josephson effect features are expected in S/STF/S and S/SBAF/S junctions, even for an equally polarized F layer. This is so, since specifying a degree of polarization is equivalent to fix the ratio of Fermi wavevectors $q_{\uparrow}/q_{\downarrow}$. However, in a SBAF and in a STF the wavevectors are different, i.e. $q_{\sigma}^{STF} \neq q_{\sigma}^{SBAF}$, and accordingly the center of mass momentum acquired by Cooper pairs will be different.

In the following, we will also consider finite temperature properties in the range $0 \leq T \leq T_c$. Even if Eq. (9) was

M		U/E_F	$m_{\uparrow}/m_{\downarrow}$
0.25	STF	8/17	1
	SBAF	0	25/9
	STF & SBAF	0.193	1.878
0.50	STF	4/5	1
	SBAF	0	9
	STF & SBAF	0.287	4.988
0.75	STF	24/25	1
	SBAF	0	49
	STF & SBAF	0.324	24.99

TABLE I: Values of the normalized exchange interaction and mass asymmetry used for three different polarization values. Here STF & SBAF represents a mixture of the two magnetic mechanism with $W = 0.5$.

derived for $T = 0$, it can be used for $T \leq T_c$, since the polarization varies only slowly on the scale of the superconducting critical temperature as long as $T_M \gg T_c$, with T_M being the Curie temperature. This condition is easily fulfilled in a typical experimental situation where the Josephson junction is realized by a ferromagnetic transition metals compound sandwiched between conventional superconductors, e.g. Niobium. In our analysis, we fix $\Delta_0 = 1$ meV and $E_F = 5$ eV, consistent with the Andreev approximation. The width of the ferromagnetic layer L is not fixed. However the maximum value used in our analysis is such that $L/\xi \approx 0.01$, such that we are in the short junction regime, corresponding to a width in the range 1–10 nm. We introduce a dimensionless parameter quantifying the scattering strength at insulating interfaces as $Z = 2mH / (\hbar^2 k)$.

Before exploring the general case, we look closer at the low polarization limit for the Andreev levels to get an idea of what to expect. Expressing the mass mismatch in a SBAF and the exchange energy in a STF as a function of polarization yields

$$\sqrt{\frac{m_{\uparrow}}{m_{\downarrow}}} = \frac{1 + M}{1 - M}, \quad (10)$$

$$\frac{U}{E_F} = \frac{2M}{1 + M^2}. \quad (11)$$

At first glance, Eqs. (10) and (11) indicate that exchange in a STF only depends on odd powers of the polarization M , while mass mismatch in a SBAF depends on all powers. Furthermore, the expansion of Eq. (10) is strictly positive, while Eq. (11) has alternating signs. Due to the intricate dependence on mass mismatch and exchange energy of the general Andreev levels Eq. (6) (see the Appendix for details), both SBAF mass mismatch and STF exchange will depend on all powers of M . However, the different sign behavior may indicate that SBAF and STF behave differently for large degrees of polarization. From now on to lighten our notation we will refer to S/SBAF/S and S/STF/S as simply SBAF and STF. The first evidence of different behavior is encountered in the $M \ll 1$, $Z \ll 1$ limit. Expanding Eq. (6) around $U/E_F \ll 1$ for STF

and $\sqrt{m_\uparrow/m_\downarrow} \approx 1$ for SBAF, we obtain

$$\varepsilon_\sigma^{\text{STF}} = \Delta_0 \left(\cos\left(\frac{\varphi}{2}\right) + \rho_\sigma \frac{kL}{2} \frac{U}{E_F} \sin\left(\frac{\varphi}{2}\right) \right) \quad (12)$$

for STF and

$$\varepsilon_\sigma^{\text{SBAF}} = \Delta_0 \left(\cos\left(\frac{\varphi}{2}\right) + \rho_\sigma \frac{kL}{2} \left(\sqrt{\frac{m_\uparrow}{m_\downarrow}} - 1 \right) \sin\left(\frac{\varphi}{2}\right) \right) \quad (13)$$

for SBAF when $Z = 0$. Then, for low polarization and including the first term from the $Z \ll 1$ -expansion, both expressions

reduce to the same form

$$\varepsilon_\sigma = \Delta_0 \left(\cos\left(\frac{\varphi}{2}\right) + \rho_\sigma M \sin\left(\frac{\varphi}{2}\right) (kL + \theta Z \sin^2 kL) \right), \quad (14)$$

where $\theta = +1(-1)$ for STF (SBAF). Thus in the low polarization regime we expect SBAF and STF to show the same behavior for $Z = 0$, while the θ -factor indicates that they can be different for nearly transparent interfaces. This is a consequence of a different interplay between the two ferromagnetic mechanisms and the insulating barrier strength described by Eq. (5). By differentiating Eq. (14) with respect to φ and inserting it into Eq. (7), we obtain the current-phase relation

$$\frac{I(\varphi)}{I_0} = 2 \frac{s_1 \sin(\varphi/2) \sinh[\beta \Delta_0 \cos(\varphi/2)] - s_2 kLM \cos(\varphi/2) \sinh[\beta \Delta_0 kLM \sin(\varphi/2)]}{\cosh(\beta \varepsilon_\uparrow/2) \cosh(\beta \varepsilon_\downarrow/2)}, \quad (15)$$

where $s_1 = \text{sgn}(\cos(\varphi/2))$, $s_2 = \text{sgn}(\sin(\varphi/2))$, and $I_0 = e\Delta_0/\hbar$. We have again put $Z = 0$ for simplicity.

From Eq. (15), we see that the current-phase relation contains a cosine term in addition to the standard sine term. One might think that the cosine term will create a non-vanishing current at $\varphi = 0, \pi$, but this is not the case. The cosine term will cancel out at $\varphi = 0, \pi$ due to the Fermi-Dirac distribution function, as shown in Eq. (15). However, in a non-equilibrium situation where levels can be differently populated, these terms may give rise to exotic features such as fractional AC Josephson effect^{43,44} or a φ -junction.⁴⁵ This possibility is matter of current investigation.

In the tunneling limit it is possible to obtain an analytical form for the current for an arbitrary degree of polarization. For $T = 0$ and including only the first term in the $Z \gg 1$ expansion, we find

$$\frac{I(\varphi)}{I_0} = \frac{1 - M^2}{1 + M^2} \frac{2 \sin(\varphi)}{Z^4 \sin\left(kL \sqrt{\frac{(1+M)^2}{1+M^2}}\right) \sin\left(kL \sqrt{\frac{(1-M)^2}{1+M^2}}\right)} \quad (16)$$

for STF and

$$\frac{I(\varphi)}{I_0} = \frac{2 \sin(\varphi)}{Z^4 \sin\left(kL \sqrt{\frac{1+M}{1-M}}\right) \sin\left(kL \sqrt{\frac{1-M}{1+M}}\right)} \quad (17)$$

for SBAF. At first glance, one may think that the main difference between the two cases is the term $(1 - M^2)/(1 + M^2)$ which is present only for STF and should damp the current for high degrees of polarization. We will later see that such an effect exists for low Z . However, for high Z this is masked by the fact that the current is small. In fact, the main difference between Eqs. (16) and (17) is that the denominator becomes wildly oscillating for large M for SBAF, but not for STF. We will see later that this effect is clearly manifested also beyond the tunneling limit.

We now move on to describe the S/F/S junction properties upon leaving aside the limits of low polarization and high/low

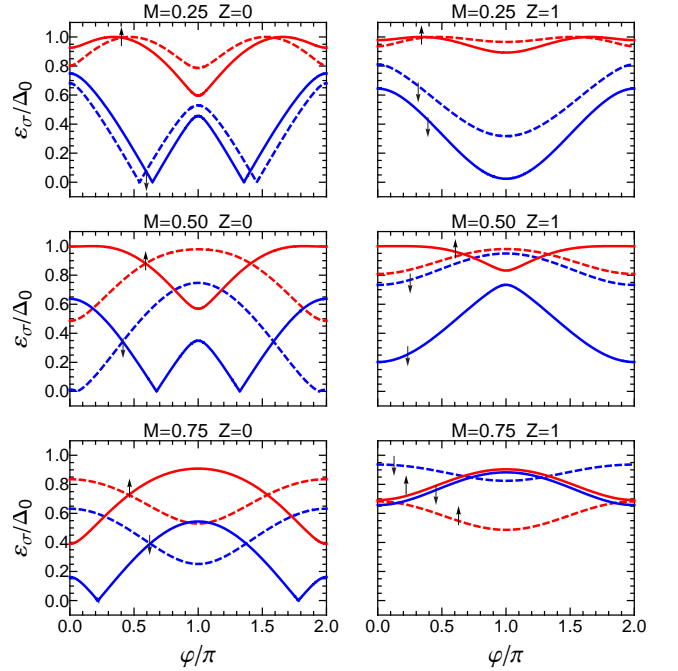


FIG. 2: (Color online). Positive branches of spin-split dispersion of the Andreev levels for different values of polarization and interface barrier strength and for $Lk = 10$, $E_F = 5$ eV, $\Delta_0 = 1$ meV. Solid lines show levels in SBAF and dashed lines in STF.

interface transparency. Fig. 2 shows the φ dependence of ε_\uparrow and ε_\downarrow in SBAF (solid lines) and STF (dashed lines) for transparent (left panels) and insulating (right panels) interfaces, for three values of polarization M . All levels are flat at $\varphi = 0, \pi$, which corresponds to the absence of Josephson current for these phase difference values. This is a well known prop-

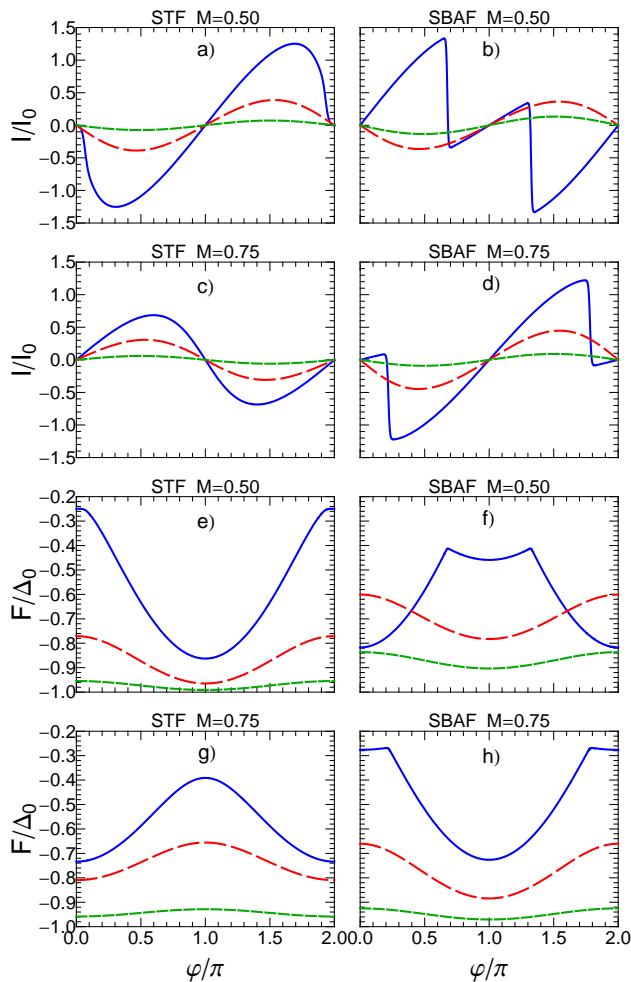


FIG. 3: (Color online). Current-phase relation and free energy for STF (left panels) and SBAF (right panels) for intermediate and high polarization values. In each panel three different interface barrier strengths are considered: $Z = 0$ (solid lines), $Z = 1$ (long-dashed lines) $Z = 2$ (short-dashed lines). Here $Lk = 10$, $E_F = 5$ eV, $\Delta_0 = 1$ meV, $T/T_c = 0.01$ are fixed.

erty of S/N/S and S/STF/S junctions, which persists in the S/SBAF/S case. However, the dispersion of the ε_σ levels are different for STF and SBAF. This difference is only quantitative for low polarizations, e.g. $M = 0.25$, as expected from Eq. (14). However, the levels differ qualitatively for higher polarization in terms of their slope and curvature. The order relation between ε_\uparrow and ε_\downarrow can also be different for the two magnetic mechanisms in the F layer, e.g. for $M = 0.75$ and $Z = 1$ $\varepsilon_\uparrow < \varepsilon_\downarrow$ for STF while $\varepsilon_\uparrow > \varepsilon_\downarrow$ for SBAF.

These differences affect the Josephson current and free energy, as shown in Fig. 3, where, I/I_0 and F/Δ_0 are plotted for different polarization values, different magnetic mechanisms, and $Z = 0$ (solid lines), $Z = 1$ (long-dashed lines), $Z = 2$ (short-dashed lines). Here $Lk = 10$, $E_F = 5$ eV, $\Delta_0 = 1$ meV, and $T/T_c = 0.01$. For low polarization values (not re-

ported in the figure) the current and the energy differ only quantitatively for STF and SBAF, while for intermediate/high polarization values a qualitative difference between the effect of the two mechanisms emerges. For instance, at $M = 0.75$ the Josephson current exhibits a maximum at $\varphi < \pi$ for STF and $\varphi > \pi$ for SBAF (see panels *c*) and *d*)). This means (as shown in panels *g*) and *h*)) that the energy minimum of the ground-state for the two types of junctions can be realized at different superconducting phase differences even though the polarization in the F layer is the same. Moreover, we see that STF is in a 0 -phase while SBAF is in a π -phase, so that the magnetic mechanism by itself is able to drive $0 - \pi$ transitions. In the following, we will refer to the situations where SBAF and STF are both in 0 - or π -phase as “in phase”, while when one is in the 0 -phase and the other is in the π -phase as “out of phase” junctions. By inspection of panel *a*), *b*), *e*), *f*) of Fig. 3 it is also possible to infer that the interface transparency can play a role in this bandwidth asymmetry driven phase shift: the STF and SBAF junctions are out of phase for $Z = 0$ and become in phase for $Z = 1, 2$, since SBAF undergoes a $0 - \pi$ transition for some Z in $[0, 1]$. We underline that STF can also undergo such transitions driven by a variation in the strength of the barrier, depending on L and T values.

In order to ascertain if the realization of out of phase junctions is a rarity or a common situation, we have compared the free energy in SBAF and STF for different width, temperature, degree of spin polarization, and interface transparency values. Our analysis shows that the condition of out of phase junctions is mainly determined by spin polarization: in the low polarization regime, i.e. $M \lesssim 0.25$, SBAF and STF junctions very often share the same phase, while in the intermediate/high polarization regime, i.e. $M \gtrsim 0.50$, they are likely to be out of phase. Other parameters only weakly affect these conditions except interface transparency which favors out of phase situation whenever the tunneling limit is considered.

We now consider the case of a mixed F with both exchange energy and bandwidth asymmetry. We show that the previously discussed features distinguishing SBAF from STF as seen in Fig. 3, are also present when considering a mixed F. Indeed the Josephson current and the free energy for mixed F look very similar to the case of a pure SBAF, when a suitable contribution of bandwidth asymmetry to total polarization is reached. Fig. 4 shows the case of a mixture of SBAF and STF with $W = 0.5$ and all other parameters fixed as in Fig. 3. In the mixed case both exchange and masses ratio have non trivial values. The values assumed by these parameters for the particular choice $W = 0.5$ are reported in Table I. As previously discussed for $M = 0.75$, STF is in a 0 -phase while SBAF is in a π -phase. It is clear from panels *b*) and *d*) of Fig. 4 that the particular mixed case considered with $W = 0.5$ is in a π -phase just like the pure SBAF case (corresponding to $W = 1$). Depending on the junctions parameters, a mixed F can behave as a pure SBAF even at smaller bandwidth asymmetry contributions. For the particular case considered here, the mixed F behaves as a pure SBAF for $W \gtrsim 0.3$. By comparing SBAF and STF at $M = 0.5$, we have pointed out that STF and is in a π -phase while SBAF is in a 0 -phase for $Z = 0$, while for smaller interface transparency SBAF switch

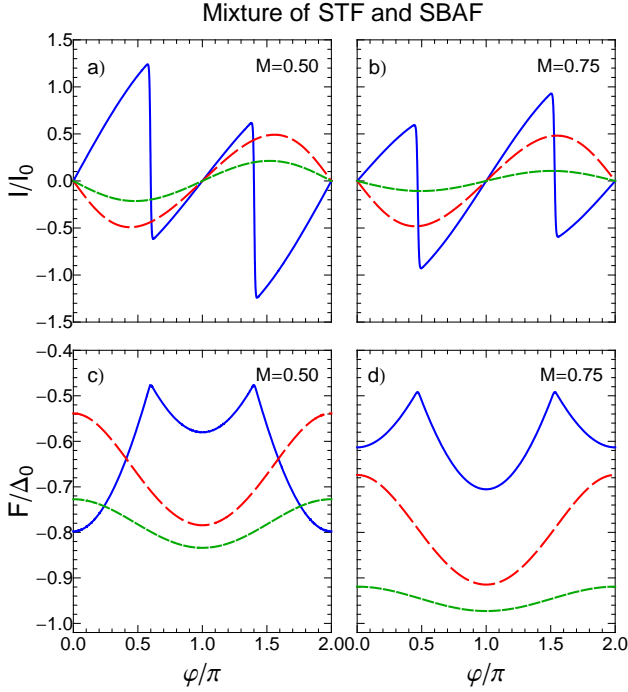


FIG. 4: (Color online). Josephson current and free energy for a ferromagnet which is a degree $W = 0.5$ mixture of STF and SBAF. All parameters are fixed at the same values of Fig. 3.

to the same phase of STF. Panels *a*) and *c*) of Fig. 4 show that even in this case a partial bandwidth asymmetry in F is enough to observe features of a pure SBAF. For the polarization considered ($M = 0.5$), a mixed F behaves as a pure SBAF for $W \gtrsim 0.4$. These results are a clear signature of the fact that the bandwidth asymmetry can induce unusual features also when it is not the only mechanism producing the spin polarization. We stress that this is an important consideration since, as discussed later, in real ferromagnetic mid-layers both exchange and bandwidth asymmetry mechanism may be present.

Fig. 5 shows the Josephson critical current as a function of L , M , and T for SBAF (solid lines) and STF (dashed lines) for $Z = 0, 1, 2$. When the L dependence is considered with a finite polarization, e.g. $M = 0.25$, the current for both the STF and SBAF junction appears oscillatory for transparent barriers and displays complicated patterns when $Z \sim 1$. These patterns repeat periodically when I_c is observed on a larger scale and collapse to a modulated Dirac comb for $Z \sim 10$. The maximum critical currents for the two junctions are very close, but they are attained for different L values and appear to be weakly affected by the Z value. The M dependence of the critical current shows a damped oscillatory behavior for SBAF and STF for $Z = 0$ and more complicated patterns for $Z = 1, 2$. The main difference between the two junctions is that for high polarization values, $M \gtrsim 0.6$, the critical current decreases monotonically for STF, whereas for SBAF it oscillates rapidly with increasing frequency. This is a signature

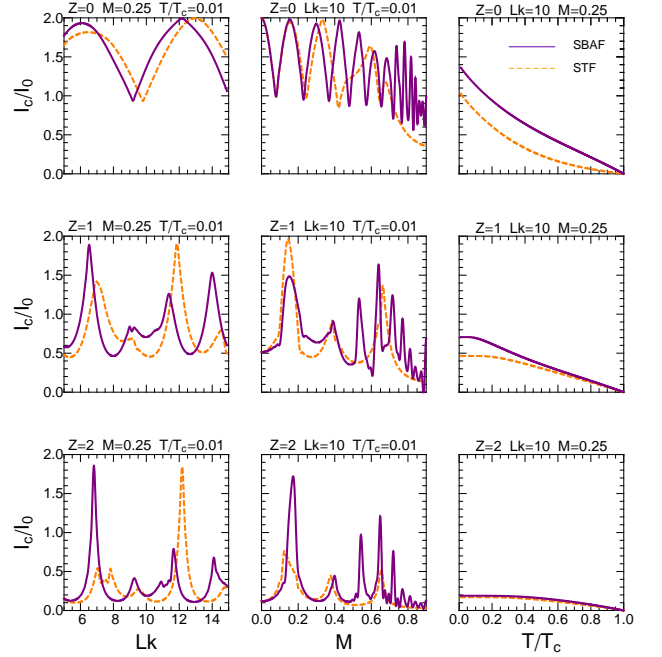


FIG. 5: (Color online). Critical Josephson current as a function of L , M , and T for SBAF (solid lines) and STF (dashed lines).

of the fact that SBAF still undergoes $0 - \pi$ transitions, while STF has settled in either a $0-$ or a $\pi-$ phase. This behavior is consistent with Eqs. (16) and (17) even if they are strictly valid only in the tunneling limit. The plots of the temperature dependence of the critical current in Fig. 5 show no particular features. The critical currents in both STF and SBAF are decaying functions of temperature, but the current in the latter junction is larger. This is not a general feature but depends on the M and L values chosen. In general one can have both $I_c^{\text{SBAF}} > I_c^{\text{STF}}$ and $I_c^{\text{SBAF}} < I_c^{\text{STF}}$ as clearly shown by the plots of critical current as a function of these parameters in Fig. 5. Moreover, a temperature driven $0 - \pi$ transition can be seen both for STF and SBAF by carefully tuning M and L ,¹⁹ e.g. $M = 0.675$, $Lk = 11.4$ for SBAF and $M = 0.935$, $Lk = 11.4$ for STF. Even a slight change in one of the two parameters suffices to destroy a temperature driven transition, and the current simply decays as in Fig. 5.

The analysis of the free energy and critical current has shown that for a given set of junction parameters such as degree of polarization, width, and insulating barrier strength, the Josephson effect in SBAF and STF can be different. These two kinds of ferromagnets can support different critical current magnitudes, can induce different ground state phases across the junction, and can undergo a different number of $0 - \pi$ transitions driven by variations in junction width and polarization. In order to study these points in more detail, it is convenient to fix a range for these parameters and then look at the behavior of STF and SBAF in this entire range. We employ this strategy because the observables are rapidly

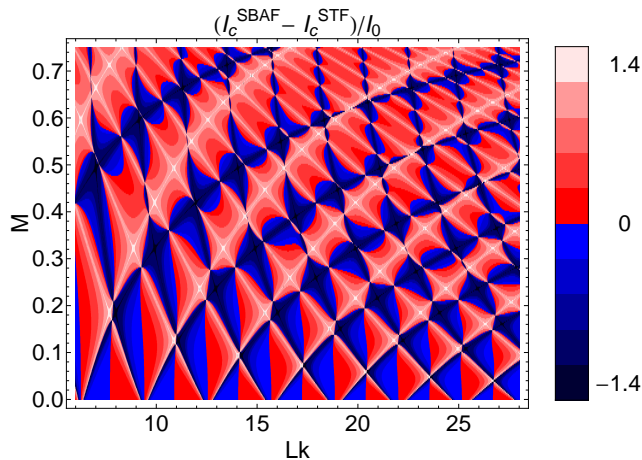


FIG. 6: (Color online). Density plot of $\Delta I = (I_c^{SBAF} - I_c^{STF})/I_0$ in the parameter range $0 < M < 0.75 \otimes 6 < Lk < 28$, and for $T = 0$ and $Z = 10$. Red-light regions are for $\Delta I > 0$. The maximum value reached is $\Delta I \simeq 1.4$. Blue-dark regions are for $\Delta I < 0$. The minimum value reached is $\Delta I \simeq -1.4$. At the borders of red and blue regions the critical currents are equal and $\Delta I = 0$.

varying functions of L and M . We here choose the parameter range $6 \leq Lk \leq 28 \otimes 0 \leq M \leq 0.75$ to be consistent with both our approximations and with typical experimental situations. First, we look at which of the ferromagnetic mechanisms that gives rise to the larger critical current, by considering the quantity $\Delta I \equiv (I_c^{SBAF} - I_c^{STF})/I_0$. This quantity is plotted for the chosen range of parameters for $T = 0$ and $Z = 10$ in Fig. 6 where red-light regions are for $\Delta I > 0$. The maximum value reached is $\Delta I \simeq 1.4$. Blue-dark regions are for $\Delta I < 0$, where the minimum value reached is $\Delta I \simeq -1.4$. At the borders of red and blue regions, the critical currents are equal and $\Delta I = 0$. The complicated pattern of ΔI shows that even a slight change in mid-layer width or polarization can reverse the order of critical current magnitudes in SBAF and STF meaning that ΔI has a strong local character. In the low polarization regime both $\Delta I < 0$ and $\Delta I > 0$ are realized with the same frequency, while in most of the intermediate/high polarization regime $\Delta I > 0$. This indicates that a SBAF is likely to support a larger critical current than a STF when considering intermediate/strong ferromagnets. This property is qualitatively independent of width, temperature, and interface transparency.

We now analyze the $0 - \pi$ transitions in the same range by plotting phase diagrams for STF and SBAF at $T = 0.01T_c$ and different values of Z (see Fig. 7). For the moment, we choose to leave aside temperature dependence, since it is not the main mechanism driving the $0 - \pi$ transitions.¹⁹

From Fig. 7 it is clear that a larger number of M and L driven $0 - \pi$ transitions is generally expected for SBAF than for STF. In particular, this is always the case for polarization driven transitions at fixed width L , regardless of the value of Z . For L -driven transitions at fixed polarization, this is the case only when $M \gtrsim 0.6$. Another point to notice is that

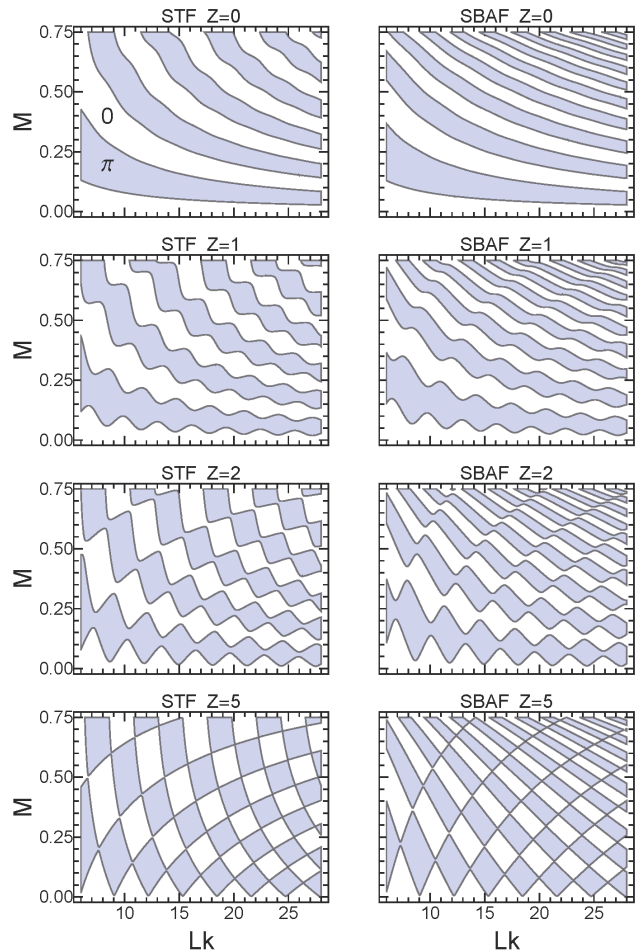


FIG. 7: (Color online). $M - L$ phase diagram for STF (left panels) and SBAF (right panels) for $T = 0.01T_c$ and different Z values. White and colored regions correspond to $0 -$ and $\pi -$ phases, respectively.

for both STF and SBAF the number of possible transitions is larger for higher Z values. At this point the origin of the complicated patterns seen in Fig. 5 for M and L dependence of I_c when $Z \neq 0$ is clear since $0 - \pi$ region boundaries become wavy for finite interface barrier strengths such that changing only M or L leaving the other fixed, boundaries can be crossed at a non-uniform frequency. We underline that the phase of the junctions manifests a strong local character and can be switched by slightly altering the width and/or the polarization.

Fig. 7 shows that SBAF undergoes more transitions than STF. It is interesting to analyze the number of transitions for a general F which can be a mixture of STF and SBAF. Fig. 8 shows the number of L driven $0 - \pi$ transitions at fixed polarization for different mixing degree W ranging from STF to SBAF. It is shown how the bandwidth asymmetry tends to

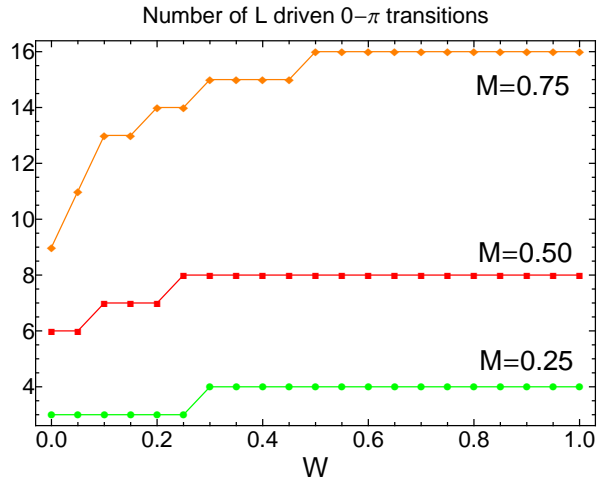


FIG. 8: (Color on line). Number of L driven $0 - \pi$ transitions in the range $6 < Lk < 28$ as a function of the relative contribution of SBAF to total polarization. $T/T_c = 0.01$ and $Z = 0$ are fixed.

increase the number of transitions and that this effect is more prominent in the high polarization regime where the number of transitions is almost doubled. One important point to note is that the same number of transitions observed in a SBAF ($W = 1$) can be observed in a mixed F whenever W is large enough, e.g. $W = 0.5$ for $M = 0.75$. This is an important point when relating our results with real materials because in experiments, one usually encounters the mixed F case. Even if $T/T_c = 0.01$ and $Z = 0$ are fixed in Fig. 7, we underline that the general trend of bandwidth asymmetry increasing the number of transitions does not depend on their particular values.

IV. CONCLUSIONS

In conclusion, we have analyzed the Josephson effect in short, ballistic single channel S/F/S junctions taking into account the possibility for ferromagnetism to be driven by a mass renormalization of carriers with opposite spin, i.e. a spin bandwidth asymmetry. We have compared a junction with this unconventional kinetically driven ferromagnetism in the F layer with one with the usual Stoner mechanism considering also their interplay. Analyzing Andreev levels, free energy and currents, we have shown that the Josephson effect in the two junctions shows different features especially for intermediate/high polarization values. In particular, we have shown that the junction with total or partial spin bandwidth asymmetry in the F layer undergoes a larger number of $0 - \pi$ transitions driven by variations in junction width and polarization. By examining free energy and phase diagrams, we have pointed out how junctions with different magnetic mechanisms in the F layer can be in different phases even if all junction parameters have the same values. We have remarked that this is a common (rare) situation in the intermediate/high (low) polar-

ization regime. By analyzing Josephson critical current we have shown that bandwidth asymmetry can both enhance and decrease its value, the former situation being more common for strong ferromagnets. Our findings are relevant for many interesting magnetic materials which cannot be framed exclusively within a Stoner scenario. As relevant examples we cite the half-metal ferromagnets defined by the property of having almost 100% transport spin polarization.⁴⁶ Materials belonging to this class usually have spin polarization M in the range where bandwidth asymmetry is clearly distinguishable from Stoner exchange, e.g. CrO_2 ,⁴⁷ $\text{La}_{0.7}\text{Sr}_{0.3}\text{MnO}_3$,⁴⁸ Fe_3O_4 ,⁴⁹ and EuO ,⁵⁰ among others. Their high polarization values cannot be ascribed only to Stoner exchange, so that when trying to theoretically model them the inclusion of bandwidth asymmetry is a fundamental ingredient.

We would like to emphasize that our findings may turn out to be useful in ascertaining if a given ferromagnetic material has spin bandwidth asymmetry. Furthermore, since a bandwidth asymmetric F layer can provide more frequent transitions and is likely to support a larger critical current for a given set of parameters than a Stoner ferromagnet, it may be more suitable for electronics or spintronics applications and devices based on the Josephson effect and relying on $0 - \pi$ transitions. Moreover, considering experimental and sample production limitations, the choice of magnetization mechanism may work as an extra degree of freedom which by itself may determine the ground state phase difference across the junction or the magnitude of Josephson critical current.

Acknowledgments

A. S. was supported by the Norwegian Research Council under Grant No. 167498/V30 (STORFORSK).

Appendix A: Explicit form of Andreev levels

The explicit form of A, B, C, D in Eq. (6) is

$$A = 2(a - b), \quad (\text{A1})$$

$$B = 4c, \quad (\text{A2})$$

$$C = 2(a + b) - d, \quad (\text{A3})$$

$$D = 2d, \quad (\text{A4})$$

where

$$a = -(\lambda_\sigma^2 + \lambda_{\bar{\sigma}}^2) - 2 \frac{\lambda_\sigma}{\tan(kL\Lambda_\sigma)} \frac{\lambda_{\bar{\sigma}}}{\tan(kL\Lambda_{\bar{\sigma}})}, \quad (\text{A5})$$

$$\begin{aligned}
b &= (1 + Z^2)^2 - Z^2 (\lambda_\sigma^2 + \lambda_{\bar{\sigma}}^2) \\
&+ (4Z^2 + 2) \frac{\lambda_\sigma}{\tan(kL\Lambda_\sigma)} \frac{\lambda_{\bar{\sigma}}}{\tan(kL\Lambda_{\bar{\sigma}})} + \lambda_\sigma^2 \lambda_{\bar{\sigma}}^2 \\
&+ 2Z(1 + Z^2) \left(\frac{\lambda_\sigma}{\tan(kL\Lambda_\sigma)} + \frac{\lambda_{\bar{\sigma}}}{\tan(kL\Lambda_{\bar{\sigma}})} \right) \\
&- 2Z \left(\lambda_\sigma^2 \frac{\lambda_\sigma}{\tan(kL\Lambda_\sigma)} + \lambda_{\bar{\sigma}}^2 \frac{\lambda_{\bar{\sigma}}}{\tan(kL\Lambda_{\bar{\sigma}})} \right), \quad (\text{A6})
\end{aligned}$$

$$\begin{aligned}
c &= (1 + Z^2) \left(\frac{\lambda_\sigma}{\tan(kL\Lambda_\sigma)} - \frac{\lambda_{\bar{\sigma}}}{\tan(kL\Lambda_{\bar{\sigma}})} \right) \\
&+ \lambda_\sigma^2 (1 + Z) \frac{\lambda_\sigma}{\tan(kL\Lambda_\sigma)} - \lambda_{\bar{\sigma}}^2 (1 + Z) \frac{\lambda_{\bar{\sigma}}}{\tan(kL\Lambda_{\bar{\sigma}})}, \quad (\text{A7})
\end{aligned}$$

and

$$d = 8 \frac{\lambda_\sigma}{\sin(kL\Lambda_\sigma)} \frac{\lambda_{\bar{\sigma}}}{\sin(kL\Lambda_{\bar{\sigma}})}, \quad (\text{A8})$$

where

$$\lambda_\sigma = \sqrt{\frac{m}{m_\sigma} \left(1 + \rho_\sigma \frac{U}{E_F} \right)}, \quad (\text{A9})$$

$$\Lambda_\sigma = \sqrt{\frac{m_\sigma}{m} \left(1 + \rho_\sigma \frac{U}{E_F} \right)}. \quad (\text{A10})$$

Appendix B: Determination of magnetic parameters for mixed F

Since the polarization is not a separable function with respect to the exchange interaction and mass mismatch, one cannot immediately obtain the values assumed by these microscopic parameters when F is a mixture of STF and SBAF. In this appendix we illustrate how we perform this calculation for a given M and W , where the mixing parameter W quantifies the relative weight of the two contributions to M . We notice that STF corresponds to $W = 0$ and SBAF to $W = 1$.

Let us consider the two dimensional $(m_\uparrow/m_\downarrow, U/E_F)$ space parameter over which M is defined (see e. g. Fig

1 of Ref.³⁴). For a given value of the polarization M , and from Eq. (11), STF is represented by the point $\left(\frac{2M}{(1+M^2)}, 0\right)$ and, from Eq. (10), SBAF is represented by the point $\left(1, \left(\frac{M+1}{M-1}\right)^2\right)$. The distance between these two points along a constant magnetization path $l(M)$ can be written as

$$\begin{aligned}
l(M) &= \frac{e^{i\pi/4}}{2\sqrt{2}} \left[B \left(-\frac{1}{4} \left(\frac{M+1}{M-1} \right)^4 ; -1/4, 3/2 \right) \right. \\
&\quad \left. - B \left(-4 \left(\frac{M^2+1}{M^2-1} \right)^4 ; -1/4, 3/2 \right) \right],
\end{aligned}$$

where B is the incomplete Euler function

$$B(z; a, b) = \int_0^z t^{a-1} (1-t)^{b-1} dt.$$

Then the coordinates in parameter space associated with a mixture defined by the actual W can be evaluated by imposing that the path between the STF and the sought points is a fraction of the total length equals to $W l(M)$. Consequently, the mass mismatch value for a degree W mixed F at polarization M can be estimated by numerically solving the equation

$$\begin{aligned}
&\frac{e^{i\pi/4}}{2\sqrt{2}} \left[B \left(f \left(\frac{m_\uparrow}{m_\downarrow}, M \right) ; -1/4, 3/2 \right) \right. \\
&\quad \left. - B \left(-4 \left(\frac{M^2+1}{M^2-1} \right)^4 ; -1/4, 3/2 \right) \right] = W l(M),
\end{aligned}$$

where

$$f \left(\frac{m_\uparrow}{m_\downarrow}, M \right) = -\frac{1}{4} \left(\frac{(M+1)^2 + \frac{m_\uparrow}{m_\downarrow} (M-1)^2}{M^2-1} \right)^4.$$

Once the sought value of mass mismatch is known, the corresponding value of exchange interaction can be obtained by inversion of Eq. (9).

¹ P. Fulde and R. A. Ferrell, Phys. Rev. **135**, 550 (1964).

² A. I. Larkin and Y. N. Ovchinnikov, Zh. Eksp. Teor. Fiz. **47**, 1136 (1964) [Sov. Phys. JETP **20**, 762 (1965)].

³ M. M. Maśka, M. Mierzejewski, J. Kaczmarczyk, and J. Spalek, Phys. Rev. B **82**, 054509 (2010).

⁴ A. Romano, M. Cuoco, C. Noce, P. Gentile, and G. Annunziata, Phys. Rev. B **81**, 064513 (2010).

⁵ R. J. Soulen Jr., J. M. Byers, M. S. Osofsky, B. Nadgorny, T. Ambrose, S. F. Cheng, P. R. Broussard, C. T. Tanaka, J. Nowak, J. S. Moodera, A. Barry, and J. M. D. Coey, Science **282**, 85 (1998); S. K. Upadhyay, A. Palanisami, R. N. Louie, and R. A. Buhrman, Phys. Rev. Lett. **81**, 3247 (1998).

⁶ R. Meservey and P.M. Tedrow, Phys. Rep. **238**, 173 (1994).

⁷ I. Žutić, J. Fabian, and S.D. Sarma, Rev. Mod. Phys. **76**, 323

(2704).

⁸ A. F. Andreev, Zh. Eksp. Teor. Fiz. **46**, 1823 (1964) [Sov. Phys. JETP **19**, 1228 (1964)].

⁹ C. W. J. Beenakker, Phys. Rev. B **46**, 12841 (1992).

¹⁰ M. J. M de Jong and C. W. J. Beenakker, Phys. Rev. Lett. **74**, 1657 (1995).

¹¹ S. Kashiwaya, Y. Tanaka, N. Yoshida, and M. R. Beasley, Phys. Rev. B **60**, 3572 (1999); Igor Zutic and Oriol T. Valls, Phys. Rev. B **60**, 6320 (1999); J. Linder and A. Sudbø, Phys. Rev. B **75**, 134509 (2007).

¹² L. N. Bulaevskii, V. V. Kuzii, and A. A. Sobyanin, JETP Lett. **25**, 290 (1977).

¹³ V. V. Ryazanov, V. A. Oboznov, A. Yu Rusanov, A. V. Veretennikov, A. A. Golubov, and J. Aarts, Phys. Rev. Lett. **86**, 2427

- (2001).
- ¹⁴ T. Kontos, M. Aprili, J. Lesueur, and X. Grison, Phys. Rev. Lett. **86**, 304 (2001).
- ¹⁵ T. Yamashita, K. Tanikawa, S. Takahashi, and S. Maekawa, Phys. Rev. Lett. **95**, 097001 (2005).
- ¹⁶ M. Chtchelkatchev, W. Belzig, Yu. V. Nazarov, and C. Bruder, JETP Lett. **74**, 323 (2001).
- ¹⁷ Z. Radovic, N. Lazarides, and N. Flytzanis, Phys. Rev. B **68**, 014501 (2003).
- ¹⁸ J. Cayssol, and G. Montambaux, Phys. Rev. B **70**, 224520 (2004).
- ¹⁹ I. Petkovic, N. M. Chtchelkatchev, and Z. Radovic, Phys. Rev. B **73**, 184510 (2006).
- ²⁰ J. Linder, T. Yokoyama, D. Huertas-Hernando, and A. Sudbø, Phys. Rev. Lett. **100**, 187004 (2008).
- ²¹ A. Millis, D. Rainer, and J. A. Sauls, Phys. Rev. B **38**, 4504 (1988).
- ²² M. Fogelström, Phys. Rev. B **62**, 11 812 (2000).
- ²³ Yu. S. Barash and I. V. Bobkova, Phys. Rev. B **65**, 144502 (2002).
- ²⁴ K. K. Likharev, Rev. Mod. Phys. **51**, 101 (1979).
- ²⁵ A. A. Golubov, M. Yu. Kupriyanov, and E. Il'ichev, Rev. Mod. Phys. **76**, 411 (2004).
- ²⁶ R. Strack, and D. Vollhardt, Phys. Rev. Lett. **72**, 3425 (1994); M. Kollar, R. Strack, and D. Vollhardt, Phys. Rev. B **53**, 9225 (1996); D. Vollhardt, N. Blümer, K. Held, J. Schlipf, and M. Ulmke, Z. Phys. B **103**, 283 (1997); J. Wahle, N. Blümer, J. Schlipf, K. Held, and D. Vollhardt, Phys. Rev. B **58**, 12749 (1998).
- ²⁷ J.E. Hirsch, Phys. Rev. B **40**, 2354 (1989); J.E. Hirsch, *ibid.* **40**, 9061 (1989); J.E. Hirsch, *ibid.* **43**, 705 (1991); J.E. Hirsch, *ibid.* **62**, 14131 (2000); J.E. Hirsch, Physica C **341-348**, 211 (2000).
- ²⁸ J.E. Hirsch, Phys. Rev. B, **59**, 6256 (1999).
- ²⁹ Y. Okimoto, T. Katsufuji, T. Ishikawa, A. Urushibara, T. Arima, and Y. Tokura, Phys. Rev. Lett. **75**, 109 (1995); Y. Okimoto, T. Katsufuji, T. Ishikawa, T. Arima, and Y. Tokura, Phys. Rev. B **55**, 4206 (1997).
- ³⁰ L. Degiorgi, E. Felder, H.R. Ott, J.L. Sarrao, and Z. Fisk, Phys. Rev. Lett. **79**, 5134 (1997); S. Broderick, B. Ruzicka, L. Degiorgi, H.R. Ott, J. L. Sarrao, and Z. Fisk, Phys. Rev. B **65**, 121102 (2002).
- ³¹ E.J. Singley, K.S. Burch, R. Kawakami, J. Stephens, D.D. Awschalom, and D.N. Basov, Phys. Rev. B **68**, 165204 (2003); E.J. Singley, R. Kawakami, D.D. Awschalom, and D.N. Basov, Phys. Rev. Lett. **89**, 097203 (2002).
- ³² Z.-J. Ying, M. Cuoco, C. Noce, and H.-Q. Zhou, Phys. Rev. B **78**, 104523 (2008); M. Cuoco, P. Gentile, and C. Noce, Phys. Rev. Lett. **91**, 197003 (2003).
- ³³ M. Cuoco, A. Romano, C. Noce, and P. Gentile, Phys. Rev. B **78**, 054503 (2008).
- ³⁴ G. Annunziata, M. Cuoco, C. Noce, A. Romano, and P. Gentile, Phys. Rev. B **80**, 012503 (2009).
- ³⁵ G. Annunziata, M. Cuoco, P. Gentile, A. Romano, and C. Noce, Phys. Rev. B, **83**, 094507 (2011).
- ³⁶ J. Kaczmarczyk and J. Spałek, Phys. Rev. B **79**, 214519 (2009).
- ³⁷ M. M. Maška, M. Mierzejewski, J. Kaczmarczyk, and J. Spałek, Phys. Rev. B **82**, 054509 (2010).
- ³⁸ P. G. de Gennes, in *Superconductivity of Metals and Alloys*, (W.A. Benjamin, Inc. New York, 1966).
- ³⁹ G. Annunziata, M. Cuoco, P. Gentile, A. Romano, and C. Noce, Supercond. Sci. Technol. **24**, 024021 (2011).
- ⁴⁰ C. W. J. Beenakker, Phys. Rev. Lett. **67**, 3836 (1991).
- ⁴¹ I. O. Kulik, Zh. Eksp. Teor. Fiz. **57**, 1745 (1969) [Sov. Phys. JETP **30**, 944 (1970)].
- ⁴² C. W. J. Beenakker and H. van Houten, Phys. Rev. Lett. **66**, 3056 (1991).
- ⁴³ H. J. Kwon, V. M. Yakovenko, and K. Sengupta, Low Temp. Phys. **30**, 613 (2004).
- ⁴⁴ J. J. A. Baselmans, T. T. Heikkilä, B. J. van Wees and T. M. Klapwijk, Phys. Rev. Lett. **89**, 207002, (2002).
- ⁴⁵ E. Goldobin, D. Koelle, R. Kleiner, and A. Buzdin, Phys. Rev. B **76**, 224523 (2007).
- ⁴⁶ I.I. Mazin, Phys. Rev. Lett. **83**, 1427 (1999).
- ⁴⁷ L. Chioncel, H. Allmaier, E. Arrighoni, A. Yamasaki, M. Daghofer, M. Katsnelson, and A. Lichtenstein, Phys. Rev. B **75**, 140406 (2007).
- ⁴⁸ B. Nadgorny, I. I. Mazin, M. Osofsky, R. J. Soulen, Jr., P. Broussard, R. M. Stroud, D. J. Singh, V. G. Harris, A. Arsenov, and Y. Mukovskii, Phys. Rev. B **63**, 184433 (2001).
- ⁴⁹ Y. S. Dedkov, U. Rüdiger, and G. Güntherodt, Phys. Rev. B **65**, 064417 (2002).
- ⁵⁰ P. G. Steeneken, L. H. Tjeng, I. Elfimov, G. A. Sawatzky, G. Ghiringhelli, N. B. Brookes, and D.-J. Huang, Phys. Rev. Lett. **88**, 047201 (2002).